Pressurized Xenon Propellant Management System for the CubeSat Ambipolar Thruster

IEPC-2015-364/ISTS-2015-b-364

Presented at Joint Conference of 30th International Symposium on Space Technology and Science, 34th International Electric Propulsion Conference and 6th Nano-satellite Symposium
Hyogo-Kobe, Japan
July 4–10, 2015

Timothy A. Collard[*], J. P. Sheehan[†] and Alec D. Gallimore[‡]
University of Michigan, Ann Arbor, MI, 48109, USA

The CubeSat Ambipolar Thruster (CAT) is nominally designed to operate on inert gas propellants with a target ΔV capability of greater than 1000 m/s. The design process for a prototype pressurized inert gas propellant feed system capable of storing enough propellant to meet this target and of delivering propellant at the flow rates of 5 - 15 sccm of xenon and pressures of 1 - 10 mbar required by CAT for an on-orbit technology demonstration mission is presented. To reduce cost and shorten development cycles, commercial-off-the-shelf (COTS) components were used and rapid manufacturing techniques were leveraged. The laser-sintered titanium propellant tank was nominally designed to store propellant at pressures up to 100 bar to exploit the supercriticality and enhanced density of xenon. The prototype tank was hydrostatically tested to 130 bar, partially validating the use of laser-sintering. The piping train comprised a three-stage pressure regulator, a low-power valve, and a standard-sized static orifice. To deliver xenon propellant at the flow rates and pressures required by CAT, a COTS orifice diameter of 40 μm was selected for integration into an engineering unit of the satellite for laboratory testing. The volume of the entire, non-optimal propulsion subsystem package is $\leq$ 2U, with the propellant tank as the primary component that can be scaled to meet the specific mission requirements, and the propellant management system mass is $\sim$ 500 g. A discussion of possible methods of optimizing the mass and volume of the propellant management system is included. Using a low thrust orbit propagator it was shown that a 3U CubeSat equipped with CAT and this propellant management system could execute a variety of orbital maneuvers, including GEO insertion, Earth escape, and orbit circularization.

Nomenclature

A = orifice area
C = a constant to account for entropic effects
$\dot{m}$ = mass flow rate
P_0 = stagnation pressure
R = gas constant
T_0 = stagnation temperature
γ = ratio of specific heats
ν = true anomaly

[*]Ph.D. Candidate, Aerospace Engineering, collardt@umich.edu
[†]Assistant Research Scientist, Aerospace Engineering, sheehanj@umich.edu
[‡]Arthur F. Thurnau Professor, Department of Aerospace Engineering. Director of the Plasmadynamics and Electric Propulsion Laboratory, alec.gallimore@umich.edu

I. Introduction

Due to standardization, modularization, and shared launch costs the CubeSat architecture, based on multiples or fractions of a cube with 10 cm sides (one 10 cm cube is 1U), has reduced costs and accelerated mission development cycles. These advantages have made CubeSats attractive options to both commercial and scientific groups that are interested in a wide range of missions types, from imaging to satellite health monitoring to space weather. Many of these missions require a level of satellite maneuverability and, therefore, a propulsion system. The exact ΔV requirements are mission dependent, but can range from less than 10 m/s to over 1000 m/s. As the interest in CubeSats has increased, a variety of chemical and electric propulsion systems have been developed, capable of ΔVs in the 100s of m/s.[1–16]

If the ΔV capabilities of CubeSat propulsion systems can be pushed above 1000 m/s, then mission and launch flexibilities will drastically increase. CubeSats would no longer be confined to their injection orbits, but could maneuver into geostationary, polar, or highly elliptical orbits. Other missions include Earth escape for deep space exploration, lunar capture from a trans-lunar trajectory (requiring ΔV between 700 and 1500 m/s depending on final orbit[17]), and orbit plane changes. Other possibilities include long-lived low altitude orbits, cluster formation flying, and the deployment of network meshes from a single launch vehicle. The CubeSat Ambipolar Thruster (CAT) is designed to bridge this technological gap.[18]

The CubeSat Ambipolar Thruster is an electrodeless, permanent magnet, helicon thruster specifically designed for the constraints of a nanosatellite. The thruster operates by coupling RF power to a plasma via a helical half-twist antenna. Due to their higher mobility the electrons leave the thruster along the field lines of the magnetic nozzle created by the permanent magnets. This charge separation establishes an electric field that then accelerates the ions. When operated on xenon flow rates of 5 - 15 sccm and power ≤ 5 W the expected thrust, I_{sp}, and efficiency are ~ 1 mN, up to 800 s, and $\sim 20\%$, respectively.[18] This high specific impulse allow ΔVs in excess of 1000 m/s to be obtained with as little as 500 g of propellant for a 5 kg, 3U CubeSat.

Xenon is an attractive propellant for CAT because of its high mass, low ionization potential, and unreactive nature. However, to store propellant mass sufficient to provide $\Delta V \geq 1000$ m/s within the CubeSat envelope xenon must be stored in pressurized tanks. To advance the development of CAT an on-orbit technology demonstration mission involving operation of CAT and the execution of maneuvers useful for future missions (spiral, orbit inclination changes, etc.) is planned. The pressurized xenon propellant management system described in this paper was designed for this CAT technology demonstration mission.

II. System Requirements

Nominally, CAT was designed to operate on a wide range of propellants, but xenon will be used for the technology demonstration mission. Xenon is the propellant of choice due to its high mass (131.3 AMU), low ionization potential (12.1 eV), and widespread use within the electric propulsion community. For the technology demonstration mission CAT is designed to integrate into a 3U CubeSat. Based on this spacecraft size the entire propulsion subsystem was required to fit into a 2U envelope. For a 5 kg, 3U CubeSat if the bus is ~ 2 kg, the CAT thruster is ~ 0.5 kg, the propellant mass is ~ 1 kg, and the mass reserved for the payload is ~ 1 kg the remaining 500 g is the maximum propellant management system dry mass. In keeping with the spirit of the CubeSat architecture, an additional design constraint of minimizing the cost of the feed system was imposed.

The propellant feed system must also be able to supply CAT with propellant at the correct conditions. To efficiently couple RF power to the plasma CAT requires the neutral propellant pressure to be 1 - 10 mbar, and, depending on the deposited power level, propellant mass flow rates of up to 15 sccm.[18] These propellant feed system requirements are summarized in Table 1.

Table 1: A summary of the propellant feed system requirements for a 3U mission with an integrated CAT.

System Requirements		Performance Requirements	
Envelope	$\leq$ 2U	ΔV	$\geq$ 1000 m/s
Dry Mass	$\leq$ 500 g	Outlet Pressure:	1-10 mbar
		Flow Rates, Xe:	5-15 sccm

III. System Design

A. Propellant Tank Design

To size the propellant tank the ideal rocket equation was used, assuming a total spacecraft mass of 5 kg. This simple formulation captured the interplay between the propellant pressure, propellant tank volume, and the expected specific impulse ranges of CAT.[18] An advantage of using xenon is that it has a low critical pressure of 58.4 bar.[19] As shown in Fig. 1, at pressures higher than this critical value xenon transitions to a supercritical fluid, accompanied by a sharp increase in the density over a small pressure range. This increased density allows for the storage of more propellant mass in the same tank volume with a small increase in pressure. By varying the specific impulse, propellant pressure, and propellant volume the applicable design space can be visualized as Fig. 2. For example, doubling the tank pressure from 40 bar to 80 bar increases the available ΔV by 550%.

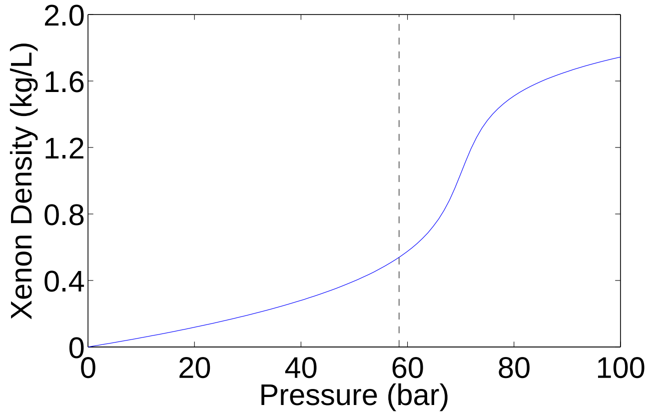

Figure 1: The density of xenon as a function of pressure, as reported by NIST.[19] The dashed line indicates the pressure at which xenon goes supercritical.

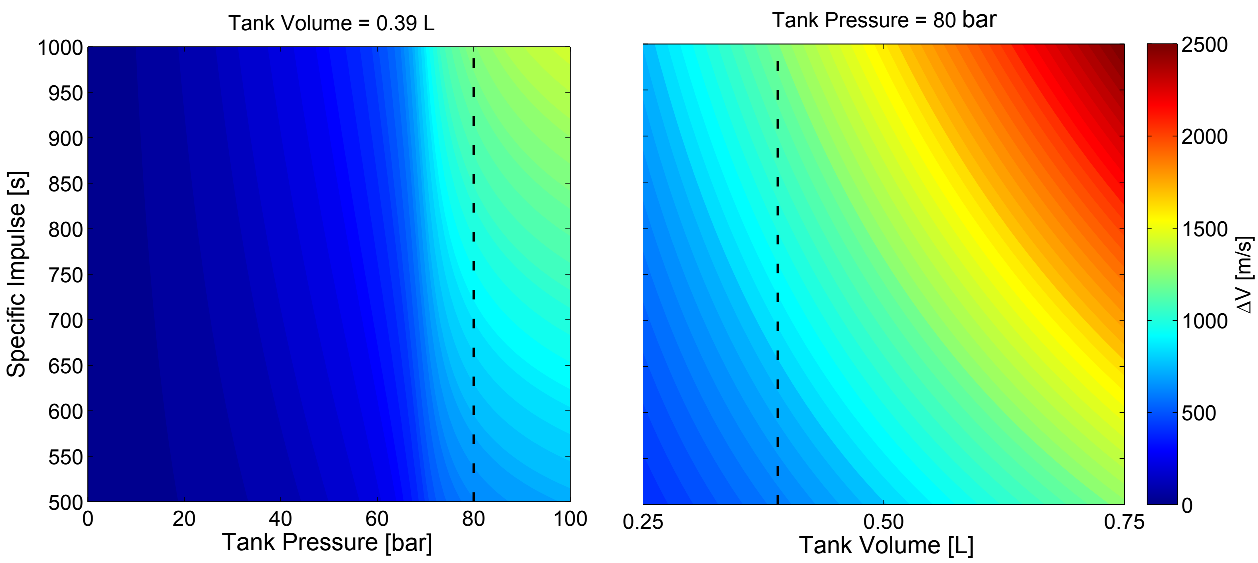

Figure 2: The ΔV provided to a representative CubeSat as a function of thruster specific impulse and xenon propellant tank pressure (left) and volume (right). The results in the left figure use a tank volume of 0.39 L and in the right figure use a tank pressure of 80 bar.

To begin to capture the benefit of using xenon the propellant must be stored at pressures above the critical pressure, as shown in Figs. 1 and 2. While the technology demonstration mission propellant management system requirements are yet to be determined a nominal tank pressure of 100 bar was selected for the propellant tank prototype. This pressure was chosen to capture the full density increase and to add margin to the anticipated propellant pressure required to meet the mission objectives.

Due to the overall system mass constraints and the pressure selection a prototype spherical titanium propellant tank was designed, with an OD of 9.5 cm and a wall thickness of 2 mm. The rapid manufacturing technique of laser-sintering titanium was chosen to accelerate the development cycle and to reduce costs. Prior to manufacturing the tank was modeled using finite element software, as shown in Fig. 3, to ensure that a minimum factor of safety of 2 was met. This factor of safety is the minimum for pressure vessels aboard Exploratory Mission 1, which is similar to the technology demonstration mission launch vehicle.[20] To account for defects due to the laser-sintering process a larger factor of safety is desirable. In this prototype design a factor of safety of 3.8 was obtained, with the minimum occurring at the joint between the tube stub and the tank due to stress concentrations. To alleviate this issue a fillet was incorporated, prior to manufacturing, thereby increasing the effective factor of safety to 5. A drawback of using titanium is that it does not readily burn up upon reentry, so reentry simulations of the final flight version of the propellant tank will need to be conducted to ensure the spacecraft poses no safety risk.

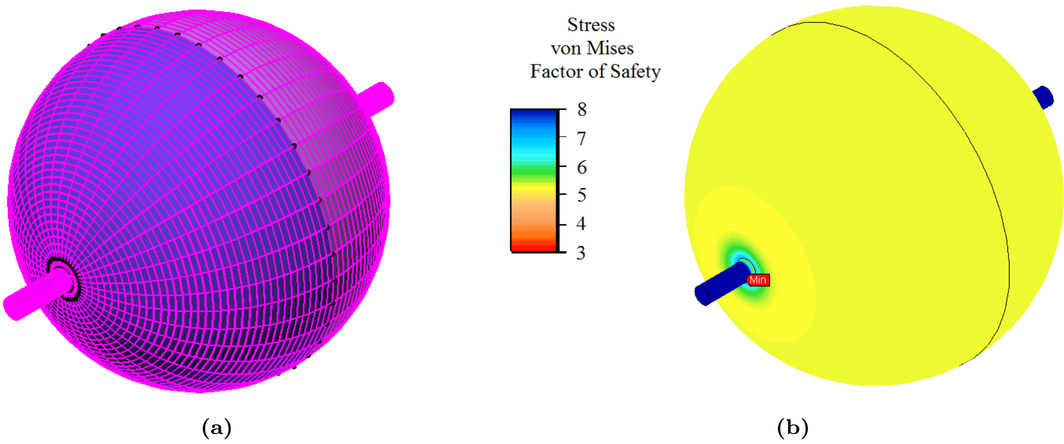

Figure 3: The a) finite element mesh and b) resulting stress factor of safety for the titanium tank with an internal pressure of 100 bar. The red arrow indicates where the minimum factor of safety was encountered.

B. Piping Train Design

To satisfy the remaining feed system requirements a series of flow elements must reduce the tank pressure to the acceptable outlet pressure range of 1 - 10 mbar and be able to deliver propellant mass flow rates of 5 - 15 sccm. Additionally, the power required to operate the system must be minimal, and the volume and mass must be minimized.

To provide repeatable CAT operation the delivered propellant pressure must be kept constant, even as the pressure within the tank decreases as propellant is consumed. To achieve this a manually adjustable COTS three-stage pressure regulator was used. This regulator was specifically designed to handle variable inlet pressures up to 200 bar, while consistently regulating to pressures to a specific setpoint within 1 - 3 bar. The overall mass of the pressure regulator is 76 g while the diameter was 1-1/32" (26.2 mm) and the height was 1-11/32" (34.1 mm).

A fixed diameter orifice is located downstream to achieve the desired flow rates. Depending on the desired propellant mass flow rate a combination of the pressure regulator setting and orifice size can be selected using choked flow theory with an empirically determined coefficient, C, that was used to account for entropic effects

$$\dot{m}_c = CP_0A\sqrt{\frac{\gamma}{RT_0}\left(\frac{2}{\gamma+1}\right)^{(\gamma+1)/(\gamma-1)}} \tag{1}$$

where $\dot{m}_c$ is the choked mass flow rate, P_0 is the stagnation pressure directly upstream of the orifice, A is the orifice area, γ is the ratio of specific heats of the propellant, R is the propellant-specific gas constant, and T_0 is the stagnation temperature. Based on the reference conditions used by the orifice manufacturer during calibration[21] for nitrogen ($\gamma = 7/5$ at room temperature) $C = 0.23$ for all choked pressure conditions and orifice areas, while for xenon ($\gamma = 5/3$ at room temperature) $C = 0.22$. Fig. 4 outlines the mass flow rates of nitrogen and xenon through a number of COTS orifice tubes for a given upstream pressure using this choked flow theory. The mass of each orifice tube was ~ 3.5 g.

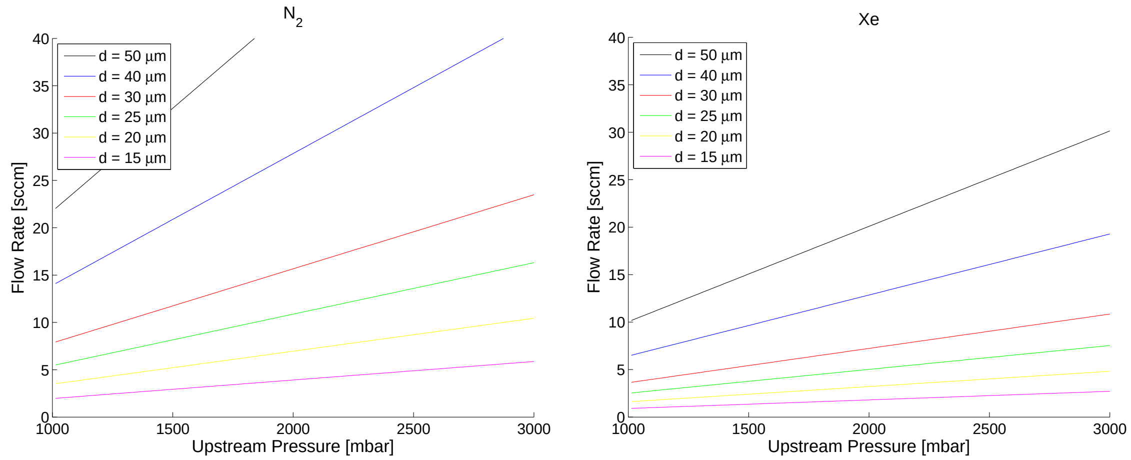

(a) **(b)**

Figure 4: The nominal expected mass flow rate of a) nitrogen and b) xenon through a given COTS orifice size with the range of pressures upstream of the orifice that the pressure regulator can deliver.

To act as an inhibit during launch and as a propellant shutoff while CAT is not operating a valve was incorporated into the system between the pressure regulator and the orifice. A COTS microfluidic valve was used, due to its small mass (4.7 g) and ability to handle the flow rates required. This valve remains closed when unpowered and required 0.25 W to open, which is small compared to the 10 - 50 W required by CAT.[18] Nominally this valve is 81.6 mm in length, including two 1.6 mm diameter 26.7 mm long inlet/outlet ports. However, the total length can easily be shortened to below 50 mm by cutting down the inlet/outlet stubs. The maximum radius, corresponding to the electrical pins, was 7.6 mm.

Based on a CAD mockup of the prototype hardware layout, Fig. 5, the system fits within the specified 2U. Not shown in the mockup is the power processing unit (PPU) that will be adjacent to the back of the thruster. While this hardware is not in its final, optimal configuration it is useful for prototype and laboratory testing. The final flight hardware will incorporate a tube stub not on the thruster centerline to reduce the unused space between the propellant tank and the thruster, reducing the overall propulsion subsystem envelope. The flight propellant tank will incorporate only a single tube stub and a fill/drain system. The final flight hardware may also use a non-spherical tank geometry to further reduce the volume of the subsystem. An all-weld piping train design will be used to reduce the number of compression fittings (potential leak sources) and reduce the mass of the propellant management system. Assuming a total piping mass of 100 g and using the masses of the components outlined above the sum total mass of the prototype propellant management system is $\sim$ 490 g, within the target dry mass of 500 g.

IV. Propellant Management System Testing

A. Propellant Tank Testing

A prototype of this laser-sintered titanium propellant tank was constructed and underwent hydrostatic testing. This tank, including the compression fittings, had a mass of 304.5 g. A hydrostatic test pump capable of nominally reaching 100 bar was used in this test. The pressure was monitored by a pressure transducer. During the test it was shown that the tank was able to withstand an instantaneous pressure of 129 bar without bursting, thereby partially demonstrating the viability of using this manufacturing process to manufacture the propellant tank. This pressure was the maximum the hydrostatic test pump was able to deliver. During testing it was observed that a small leak formed on one of the tube stub compression fittings due to a manufacturing defect that caused a flat spot on the tank tube stub. To remedy this issue future propellant tanks will incorporate tube stubs that have oversized ODs that will be turned down to tight tolerances using a lathe. Future tests will pressurize a similar tank to 200 bar.

B. Piping Train Testing

To determine the combination of pressure regulator setting and orifice size required for a given propellant mass flow rate, a pressure transducer was integrated between each of the major components (regulator, valve, and orifice), as shown in Fig. 6. This also serves to measure the outlet pressure. Using the pressure transducers bracketing the orifice, the mass flow rate was calculated using choked flow theory.

The orifice was located downstream of the valve to prevent excessive propellant loss and unanticipated thrusting upon opening the valve due to draining of the high-pressure propellant within the dead volume between the orifice and valve. In this configuration, the volume between the valve and the orifice filled and reached a steady pressure within $\sim$ 5 s of valve actuation. The bypass line was used to quickly evacuate the volume upstream of the orifice between valve actuations and pressure regulator adjustments. Due to the low flow rates, especially at the smaller orifice diameters ($d \leq 20\ \mu$m), the time to deplete the propellant in this volume was on the order of 10s of minutes. For a flight version of this feed system this equates to unsteady thrust that is unaccounted for at the end of propulsive maneuvers and an unnecessary waste of propellant in an unwanted cold gas discharge. Therefore, this volume must be minimized.

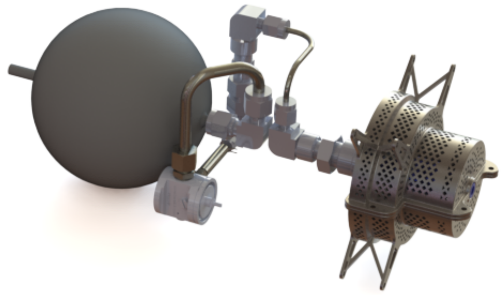

Figure 5: A notional propulsion system layout, using prototype hardware, for integration into a CubeSat bus to check the envelope requirement.

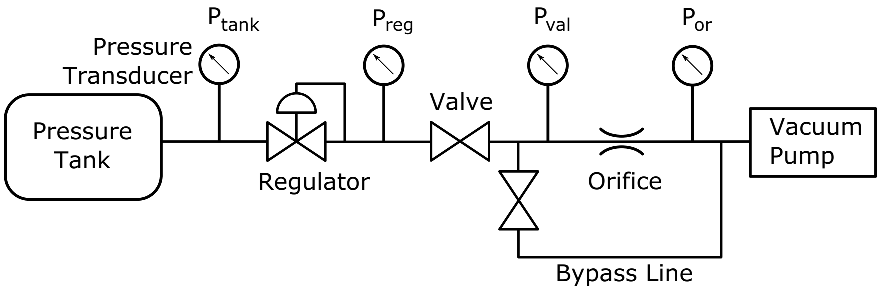

Figure 6: A schematic of the propellant feed system characterization experimental setup.

For initial testing, N_2 was used to reduce cost and the ambient temperature (and gas temperature) was 293 K. The critical parameter for determining the propellant flow rate through the piping train, for a fixed orifice area, was the pressure upstream of the orifice. As shown in Fig. 7 the steady-state pressure directly upstream of the orifice varied nearly linearly with the regulated pressure setting, which implies a nearly constant pressure drop through the system. This was reasonable for a system that was choked at the orifice and quickly reaches an equilibrium, steady-state pressure during operation. The linearity, even with varying orifice size, also demonstrates good system repeatability, which will be essential for laboratory testing of the final, integrated propulsion subsystem.

Given that the pressure drop and flow across an orifice was highly dependent on the pressure upstream, other pressure drops within the feed system can alter the performance. The main potential source of pressure drop upstream of the orifice is the valve, so the inlet and outlet pressures must be measured. Since the two pressures were equal within error bars, as shown in Fig. 8, the effective pressure drop across the valve was negligible. This implies that the volume upstream of the orifice was filled with propellant and that propellant flow through the orifice was immediately replenished by propellant further upstream. Note that the pressure ratio is marginally less than one because the error bars are dependent on the full-scale pressure range, which was higher for P_{reg}. The slight changes in the pressure ratio were likely due to small nonlinearity errors in the pressure transducers, especially in the low end of P_{reg}.

The flow rate was inferred from the pressures upstream of the orifice using Eq. 1. Based on the pressure difference across the orifice the choked condition was always met. Using the COTS calibrated orifice sizes

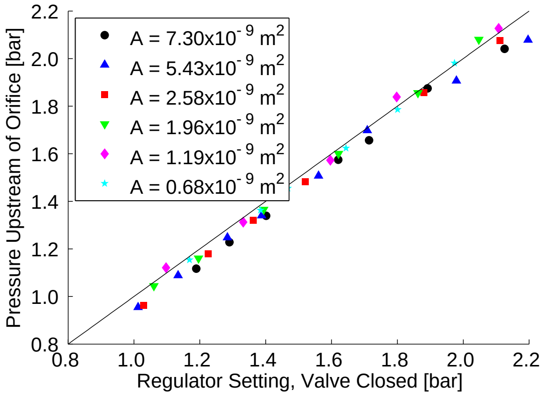

Figure 7: The pressure upstream of the orifice when propellant is flowing through the system compared to the actual regulated pressure setting.

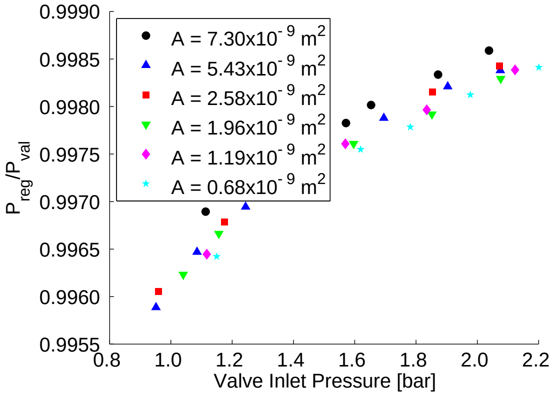

Figure 8: The pressure at the inlet and outlet of the valve. Since the two are equal, within error bars, the effective pressure drop across the valve is negligible.

tested ($d = 15 - 50$ μm) the piping train system could provide propellant flow rates of 2 - 50 sccm on N_2 and therefore the flow rates required for CAT operation. Like the downstream pressure there was some overlap in the flow rate capabilities of similarly sized orifices, enhancing the flexibility of the system. While this flexibility may be useful in providing conditions for optimal CAT operation, it is generally advisable to minimize the pressure regulator setpoint because as the pressure within the tank falls to this level the feed system will begin providing propellant at off-design conditions.

The important parameters for CAT are the pressure downstream of the orifice, Fig. 9, and the propellant flow rate, Fig. 10. The pressure downstream of the orifice is directly measured by a pressure transducer, and falls within the required range of 1 - 10 mbar. The variations in the downstream pressure due to changes in the orifice diameter may have slight impacts on the precise power and frequency conditions required for optimal CAT performance.

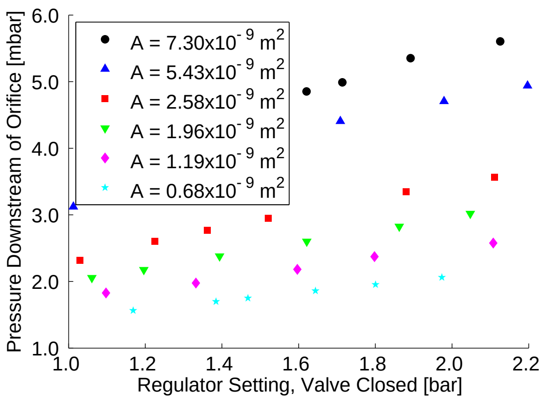

Figure 9: The pressure downstream of the orifice when propellant is flowing through the system compared to the actual regulated pressure setting.

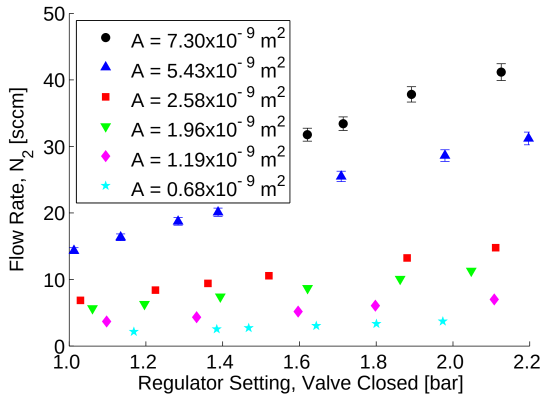

Figure 10: The flow rate of N_2 when propellant is flowing through the system compared to the actual regulated pressure setting. Data points without error bars have uncertainty ranges smaller than the size of the point.

For the CAT technology demonstration mission, after correcting for the differences between nitrogen and xenon flow rates, the orifice size of 5.43x10^{-9} m^2 (orifice diameter of 40 μm) was selected because it best covers the 5 - 15 sccm range while remaining within 1 - 10 mbar. This flow rate coverage will allow for the development of a single engineering unit for laboratory testing using a single integrated orifice size and rapid testing of the full CAT operational envelope by changing only the pressure regulator setting. It is important to note that the flight orifice area may vary slightly from the reported value because the orifice manufacturer does not produce perfectly circular orifices, rather a nominal laser-cut diameter size with tolerances of $\pm$ 5% is selected and the manufacturer reports the effective diameter found during calibration. In the event that final mission requirements dictate a combination of propellant flow rates and system pressures not possible using these COTS orifices custom sizes can be produced, but would increase the overall system cost.

V. Example Orbital Maneuvers

By integrating this propellant management system and CAT into a CubeSat a number of useful orbital maneuvers become possible. With the proposed 0.39 L spherical tank design filled with xenon pressurized to 80 bar the onboard propellant mass is $\sim$ 0.65 kg. For the non-spherical flight tank geometries being considered the propellant mass can be increased to $\sim$ 1.5 kg. To investigate the envelope of possible maneuvers, including orbit circularization and geostationary (GEO) orbit insertion, a low thrust orbit propagator was used. Throughout all simulations an I_{sp} of 800 s, total spacecraft wet mass of 5 kg, and xenon flow rate of 5 sccm (corresponding to a mass flow rate of 0.5 mg/s and an ideal power consumption of 31 W) was assumed. These conditions are suitable for CubeSats that are intermittently firing or have deployable solar arrays.

For a number of CubeSat missions, including Earth and space-weather monitoring and the deployment of communication arrays, orbit circularization is a useful maneuver. An arbitrary initial CubeSat deployment orbit with perigee at an altitude of 500 km and apogee at 1600 km was chosen for this maneuver. The final circular orbit at an altitude of 500 km was reached by firing CAT retrograde when the spacecraft was near perigee ($|\nu| \leq 15°$, where ν is the true anomaly). Based on these parameters this maneuver required a ΔV of $\sim$ 280 m/s, consumed 0.17 kg of propellant, and was completed in $\sim$ 55 days. The orbital trajectory for this maneuver is found in Fig. 11a. If the 0.39 L spherical tank had been used this maneuver would have consumed $\sim$ 25 % of the total available propellant mass, leaving sufficient mass for station-keeping and other maneuvers. This type of maneuver, due to its low propellant consumption, increases the flexibility of the initial CubeSat deployment orbit, thereby lowering launch costs. This maneuver is also similar to an orbit lowering maneuver that can accelerate end-of-life timelines and reduce in-space debris.

CubeSats are also suitable for monitoring the health of larger, more expensive satellites. If sufficient ΔV is available these monitoring missions could include satellites parked in GEO. To simulate this mission a GEO insertion maneuver from a geostationary transfer orbit (GTO) with a perigee altitude of 300 km and an apogee altitude of 35,800 km was investigated. To insert into GEO from this orbit CAT was fired prograde when near apogee ($|\nu| \geq 175°$) to raise perigee to GEO and then retrograde when near perigee ($|\nu| \leq 5°$) to circularize the orbit. Based on these parameters this maneuver required a ΔV of $\sim$ 1500 m/s, consumed 0.86 kg of propellant, and was completed in $\sim$ 6 months. A visual representation of this maneuver is found in Fig. 11b. While this required propellant mass exceeds the maximum mass available using the spherical tank it is well within the range of the non-spherical flight tank designs being considered. To deorbit from GEO an $\sim$ 8 month spiral maneuver back to a 300 km perigee altitude could be performed using $\sim$ 0.5 kg of propellant. For GEO the required ΔV for station-keeping is $\sim$ 50 m/s per year.[22] If a full GEO CubeSat mission using a non-spherical tank with 1.5 kg of propellant was executed, including the the insertion and deorbit maneuvers, a GEO orbit could be maintained for $\sim$ 5 years. In addition to health monitoring missions this series of maneuvers would allow for other missions to GEO including Earth observation and communications relaying.

With sufficient ΔV CubeSats become capable of missions to near-Earth objects or other planets. The first maneuver for these missions is Earth-escape. To investigate the feasibility of this type of maneuver using CAT a spiral maneuver from GTO with a perigee altitude of 300 km and an apogee altitude of 35,800 km was simulated, including lunar perturbations. The maneuver was completed when the apogee reached the limit of the sphere-of-influence of Earth (925,000 km). To execute this maneuver CAT was fired prograde relatively near perigee ($|\nu| \leq 70°$) during each orbit. If the perigee altitude fell below 300 km CAT was also fired prograde near apogee ($|\nu| \geq 175°$). Based on these parameters this maneuver required a ΔV of $\sim$ 980 m/s, consumed 0.59 kg of propellant, and was completed in $\sim$ 2.3 years. A visual representation of this maneuver is found in Fig. 11c. While this maneuver is possible with the 0.39 L spherical tank it would have consumed $\sim$ 91 % of the available propellant, leaving little for the remainder of the mission. A non-spherical tank geometry that could store more propellant would enable further maneuvering.

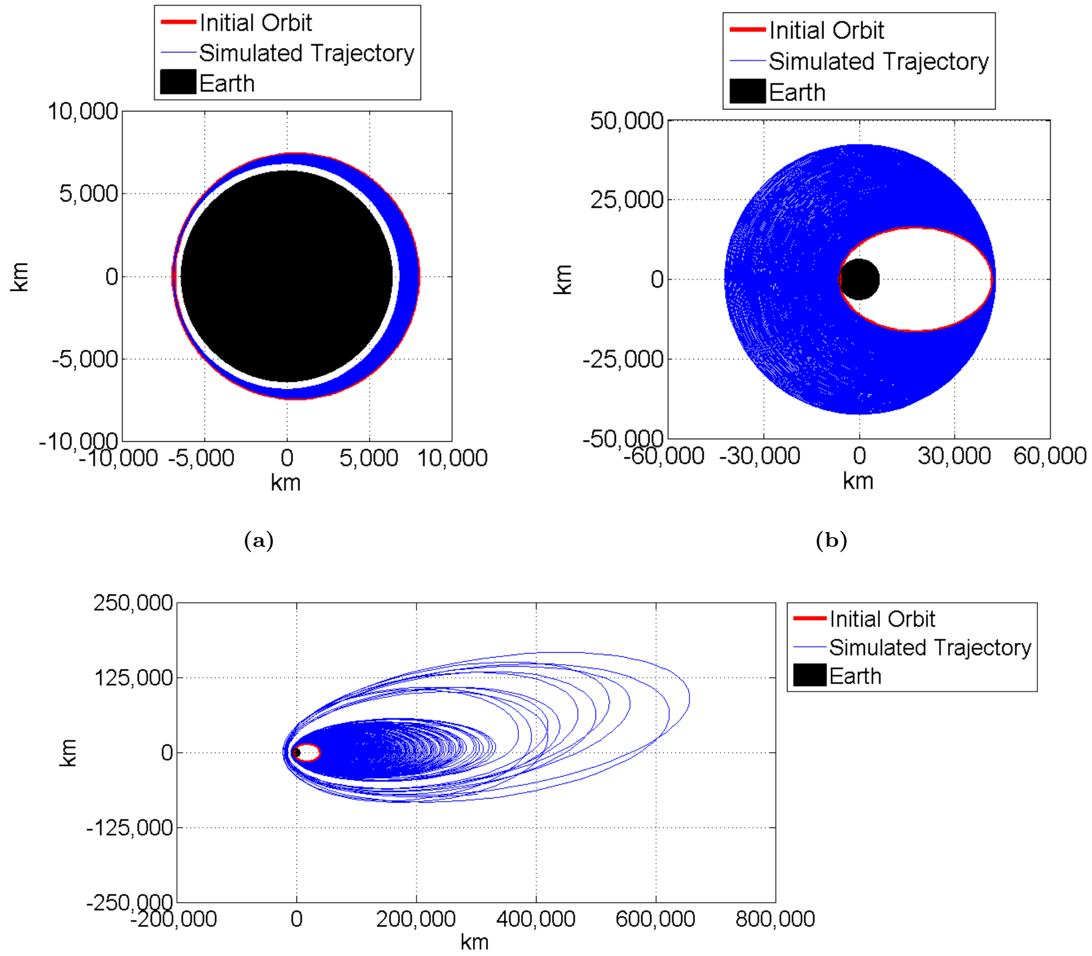

(a) (b) (c)

Figure 11: Example spacecraft maneuvers using CAT and a propellant management system similar to the one outlined in this paper. a) An example orbit circularization maneuver. b) An example GTO to GEO insertion maneuver. c) An example Earth escape maneuver with lunar perturbations.

VI. Conclusions

A pressurized inert gas propellant feed system leveraging COTS components is presented. A low cost laser-sintered titanium propellant tank was designed to accommodate propellant pressures of up to 100 bar, and initial hydrostatic tests indicate that using laser-sintering manufacturing techniques is a viable option for pressure vessels. Using such manufacturing techniques reduce cost and accelerates the development cycle for custom, mission-specific components. These benefits enable low budget missions and allow for a wider range of contributors to in-space science, including small businesses and university teams.

A piping train comprised a pressure regulator, valve, and static orifice delivers propellant at the pressure and flow rate conditions required by CAT for the technology demonstration mission, with an orifice area of 5.43E-9 m^2 (orifice diameter of 40 μm) capable of providing nearly the full 5 - 15 sccm xenon flow rate range. The entire propulsion subsystem fits within a 2U envelope, with the propellant tank the main scalable component to meet specific mission requirements. The flexibility of this propellant management system is enhanced by the system simplicity, low cost, and low power consumption. By integrating multiple parallel orifices it is possible to add system redundancy or allow for on-orbit switching of CAT operational modes. With small modifications to this simple system it is also possible to use this propellant management system with other thrusters or a range of missions requiring different CAT operating conditions, including missions that Earth escape, GEO insertion, and orbit circularization maneuvers.

VII. Acknowledgements

This material is based upon work supported by the National Aeronautics and Space Administration under Award No. NNX14AD71G. The authors would like to thank Arun Nagpal and David Hash for their technical assistance.

References

[1] Derek Schmuland, Robert Masse, and Charles Sota. Hydrazine propulsion module for cubesats, 2011.

[2] Derek Schmuland, Christian Carpenter, Robert Masse, and Jonathan Overly. New insights into additive manufacturing processes: Enabling low-cost, high-impulse propulsion systems, 2013.

[3] Aaron Dinardi and Mathias Persson. High performance green propulsion (hpgp): a flight-proven capability and cost game-changer for small and secondary satellites, 2012.

[4] F Trezzolani, A Lucca Fabris, D Pavarin, A Selmo, and M Manente. Low power radio-frequency plasma thruster development and testing, 2013.

[5] Andrew Bertino-Reibstein and Adam Wuerl. Development of a warm-gas butane system for microsatellite propulsion, 2013.

[6] Igal Kronhaus, Klaus Schilling, Satish Jayakumar, Alexander Kramer, Mathias Pietzka, and Jochen Schein. Design of the uwe-4 picosatellite orbit control system using vacuum-arc-thrusters. In *Proceedings of the 33rd International Electric Propulsion Conference*, pages 2013–195.

[7] Shingo Fuchikami, Masayoshi Nakamoto, Kazuhiro Toyoda, and Mengu Cho. Development of vacuum arc thruster for nano-satellite. In *33rd International Electric Propulsion Conference, Washington DC, USA*.

[8] Alexey Shashurin, Michael Keidar, and Taisen Zhuang. Comparative analysis of micro-cathode arc thruster performance, 2013.

[9] Taisen Zhuang, Alexey Shashurin, Isak Beilis, and Michael Keidar. Ion velocities in a micro-cathode arc thruster. *Physics of Plasmas (1994-present)*, 19(6):063501, 2012.

[10] Francois Martel, Louis Perna, and Paulo Lozano. Miniature ion electrospray thrusters and performance test on cubesats, 2012.

[11] Douglas Spence, Eric Ehrbar, Nate Rosenblad, Nate Demmons, Tom Roy, Samuel Hoffman, Dan Williams, Vlad Hruby, and Chris Tocci. Electrospray propulsion systems for small satellites, 2013.

[12] MS Rhee, CM Zakrzwski, and MA Thomas. Highlights of nanosatellite propulsion development program at nasa-goddard space flight center, 2000.

[13] M Coletti, F Guarducci, and SB Gabriel. A micro ppt for cubesat application: Design and preliminary experimental results. *Acta Astronautica*, 69(3):200–208, 2011.

[14] Andrew D Ketsdever, Riki H Lee, and Taylor C Lilly. Performance testing of a microfabricated propulsion system for nanosatellite applications. *Journal of Micromechanics and Microengineering*, 15(12):2254, 2005.

[15] Donald Platt. A monopropellant milli-newton thruster system for attitude control of nanosatellites, 2002.

[16] Nathan Orr, Jesse Eyer, Benoit Larouche, and Robert Zee. Precision formation flight: the canx-4 and canx-5 dual nanosatellite mission, 2007.

[17] David Folta, Donald Dichmann, Pamela Clark, Amanda Haapala, and Kathleen Howell. Lunar cube transfer trajectory options. 2015.

[18] J. P. Sheehan, Collard Timothy, W. Longmier Benjamin, and Reese Ingrid. *New Low-Power Plasma Thruster for Nanosatellites*. Propulsion and Energy Forum. American Institute of Aeronautics and Astronautics, 2014. doi:10.2514/6.2014-3914.

[19] E.W. Lemmon, M.O. McLinden, and D.G. Friend. "thermophysical properties of fluid systems" in nist chemistry webbook, nist standard reference database number 69.

[20] NASA. Space launch system (sls) secondary payload user's guide (spug). (SLS-SPIE-HDBK-005), 2015.

[21] R.R. Gidner. Fluid flow through calibrated orifices. http://www.lenoxlaser.com/publication/Fluid%20flow%20through%20calibrated%20orifices.pdf. Accessed: 2015-03-31.

[22] E. M. Soop. *Handbook of geostationary orbits*. Space technology library ;v. 3. Kluwer Academic Publishers ; Microcosm, Dordrecht; Boston: Torrance, Calif., 1994.